Proceedings of Global Power and Propulsion Society
ISSN-Nr: 2504-4400
GPPS Xi'an21
18th – 20th October, 2021
www.gpps.global

GPPS-TC-2021-0345

Unsteady Analysis with Throughflow Concept

Yinbo Mao
Tsinghua University
yimao@mail.tsinghua.edu.cn
Beijing, China

Xinrong Su
Tsinghua University
suxr@mail.tsinghua.edu.cn
Beijing, China

Xin Yuan
Tsinghua University
yuanxin@mail.tsinghua.edu.cn
Beijing, China

ABSTRACT

This paper presents a thoroughly derived theory that incorporates unsteady formulations into standard throughflow methods such that certain transient characteristics can be captured by throughflow analysis. In analogy to the relation between conventional throughflow methods and the mixing plane concept, this paper proposed a novel approach of quantifying the unsteadiness by relating the throughflow method to the chorochronic interface. Maintaining the advantage of low computational cost inherited from throughflow methods, the new method has huge potentials in the unsteady design of turbomachineries.

INTRODUCTION

Unsteady analysis of turbomachineries is a topic of everlasting interest over the past half a century. Unlike the standard steady aerodynamic analysis, the unsteady analysis is of significant complexity due to various flow structures, e.g. vortex shedding and jet interactions etc., within the flow field, making it extremely difficult to understand the flow qualitatively, let alone to quantify it. To the interest of researchers and engineers in this area, the unsteady aerodynamic analysis is useful in two aspects: noise evaluation and flow stability evaluation. Mathematically speaking, the former focuses on the high-frequency unsteadiness that associates with blade-row interactions such as jet flow, vortex shedding and turbulence. Such unsteadiness usually has a length scale of fractions of the blade pitch and generates tonal and buzz-saw noises that have been investigated with some serious endeavours (Envia, 1994). The latter, on the other hand, are more about the operating range of turbomachineries. The process of instability of compressors, namely the development of rotating stalls, is a typical unsteady process. However, the length scale of such unsteadiness is on the order of several pitches (Day, 1993), which is much larger compared to the noise-related unsteadiness.

Common approaches to study unsteadiness in turbomachineries are experiments and high-fidelity CFD simulations (Denton 1975, 1992; Daws, 1988; He, 1997). Both approaches are expensive when full-wheel subjects are involved. Many researchers have made attempts trying to reduce the computational cost of unsteady full-wheel simulations (Gerolymos, 2013; He, 2010). Analogous to the mixing plane in steady flow proposed by Denton (1992), a chorochronical interface (Gerolymos, 2002) coupled with Fourier analysis (He, 1990) is utilized in unsteady flow analysis to simplify the simulations setting. However, for the preliminary design of compressors, such a level of cost reduction is still not acceptable. Hence the present paper is seeking to develop a more efficient model, based on the outstanding ideas from precedent scholars, for unsteady analyses of turbomachineries.

The basic concept, to begin with, is the throughflow model. Originating from the quasi-3D theory (Wu, 1952), the streamline curvature method (SLC) has been widely used in various applications in turbomachinery in the past few decades (Novak 1967; Jennions and Stow, 1985a, 1985b; Casey and Robinson, 2010). Later the development of computer science prompts the development of CFD-based throughflow (Spurr, 1980; Damle et al., 1997; Sturmayr and Hirsch, 1999), which shows tremendous advantages in handling transonic turbomachines. These throughflow methods model uniform-inlet flows with axisymmetric simulations at a very low computational cost. It, however, also limits its usage for higher-dimensional aerodynamic problems such as inlet distortions. To extend the usage of throughflow to 3D flows, researchers proposed various solutions such as the parallel compressor model (Mazzawy, 1977; Peters et al., 2015) and the 3D throughflow modelling (Mao and Dang, 2020). Regardless, the throughflow modelling remains in the steady-flow regime.

Recently, there have existed endeavours to incorporate unsteady modelling into the framework of blade-less simulation (Longley 2007; Righi et al., 2017; Guo et al., 2020). This line of work focused on taking the first-order linearization of transient terms and extend pre-existing steady models to unsteady formulations. Though being effective, these researches are based on axisymmetric bode-force modelling. Given that the throughflow concept has been extended to 3D (Mao and Dang, 2020), it will be interesting if the unsteady modelling can be incorporated into the framework of the 3D throughflow method.

Considering the averaging nature of throughflow methods, it is theoretically feasible to use throughflow to address large-scale modal waves and unsteady signals in the flow field. Based on this deduction, the authors will try to derive the governing equations for unsteady throughflow modelling for turbomachineries. The starting point of derivation is the unsteady Reynolds Averaged Navier-Stokes (RANS) equations. With the basic idea of throughflow and the unsteady characteristics in multi-row machines, governing equations of the passage-average flow quantities will be derived and discussed.

GOVERNING EQUATION

The subject of research is any standard multi-row stages. Here a turbine stage is taken as an example and the schematic is shown in Figure 1.

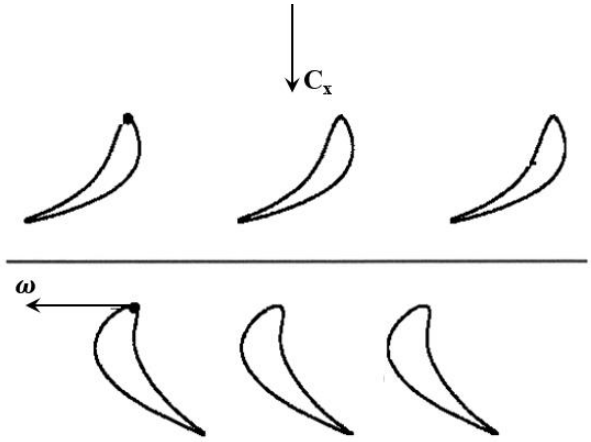

Figure 1 Schematic of a two-row stage.

The final goal is to use throughflow to model the flow with such a stage, preserving substantial large-scale unsteadiness. Therefore, one should not use the 3D throughflow method, treating rotating and stationary rows all in the lab frame (Adamczyk, 1989; Mao and Dang, 2020), as the unsteadiness may not be preserved in the averaging process. As a result, the target method should address the nozzle and the rotor in different frames. This brings the concept of the chorochronical interface that combine unsteady calculations in different frames.

Taking the nozzle as an example, the starting point is the URANS equations along with the continuity and energy equations in the absolute frame. If one writes them in components in the cylindrical coordinates, these equations become

$$\frac{\partial \rho}{\partial t}+\frac{\partial \rho V_x}{\partial x}+\frac{1}{r}\frac{\partial r\rho V_r}{\partial r}+\frac{1}{r}\frac{\partial \rho V_\theta}{\partial \theta}=0 \tag{1}$$

$$\frac{\partial \rho V_x}{\partial t}+\frac{\partial \rho V_x V_x}{\partial x}+\frac{1}{r}\frac{\partial r\rho V_x V_r}{\partial r}+\frac{1}{r}\frac{\partial \rho V_x V_\theta}{\partial \theta}=-\frac{\partial p}{\partial x}+F_{\tau x} \tag{2}$$

$$\frac{\partial \rho V_r}{\partial t}+\frac{\partial \rho V_r V_x}{\partial x}+\frac{1}{r}\frac{\partial r\rho V_r V_r}{\partial r}+\frac{1}{r}\frac{\partial \rho V_r V_\theta}{\partial \theta}-\frac{\rho V_\theta V_\theta}{r}=-\frac{\partial p}{\partial r}+F_{\tau r} \tag{3}$$

$$\frac{\partial \rho V_\theta}{\partial t}+\frac{\partial \rho V_\theta V_x}{\partial x}+\frac{1}{r}\frac{\partial r\rho V_\theta V_r}{\partial r}+\frac{1}{r}\frac{\partial \rho V_\theta V_\theta}{\partial \theta}+\frac{\rho V_r V_\theta}{r}=-\frac{1}{r}\frac{\partial p}{\partial \theta}+F_{\tau\theta} \tag{4}$$

$$\frac{\partial \rho h_0}{\partial t}+\frac{\partial \rho h_0 V_x}{\partial x}+\frac{1}{r}\frac{\partial r\rho h_0 V_r}{\partial r}+\frac{1}{r}\frac{\partial \rho h_0 V_\theta}{\partial \theta}=\frac{\partial p}{\partial t}+\vec{F}_\tau\cdot\vec{V}+D+Q \tag{5}$$

$$p=\rho RT \tag{6}$$

To derive governing equations for throughflow methods, it is essential to perform average operations. Here the moving average used by Mao and Dang (2020) is adopted. That is, for an arbitrary quantity ϕ, the moving average (Hyndman, 2011) over one pitch is defined as

$$\hat{\phi} = \frac{N}{2\pi B}\int_{\vartheta}^{\vartheta+\frac{2\pi}{N}} G\phi d\theta \tag{7}$$

The G in Equation (7) is a gate function that is defined as

$$\left.\begin{array}{c} G = U(\theta - \vartheta) + U\left(\theta - \vartheta - \theta_{\mathrm{p}}\right) - U(\theta - \vartheta - \theta_{\mathrm{s}})(in\ passage) \\ G = 1\ (outside\ passage) \end{array}\right\} \tag{8}$$

The B in Equation (7) is the blockage factor defined as

$$B = \begin{cases} 1 - \dfrac{\left(\theta_{\mathrm{p}} - \theta_{\mathrm{s}}\right)N}{2\pi}(in\ passage) \\ 1\ (outside\ passage) \end{cases} \tag{9}$$

By applying Equation (7) to Equations (1) through (5), the resultant governing equations become

$$\frac{\partial B\hat{\rho}}{\partial t} + \nabla\cdot\left(B\hat{\rho}\vec{\tilde{V}}\right) = 0 \tag{10}$$

$$\frac{\partial\hat{\rho}\vec{\tilde{V}}}{\partial t} + \hat{\rho}\vec{\tilde{V}}\cdot\nabla\vec{\tilde{V}} = -\nabla(\hat{p}) + \frac{\vec{F}_b}{B} + \vec{\hat{F}}_{\tau} + \vec{P} \tag{11}$$

$$\frac{\partial\hat{\rho}\breve{h}_0}{\partial t} + \bar{\rho}\vec{\tilde{V}}\cdot\nabla\breve{h}_0 = \frac{\partial\hat{p}}{\partial t} + \frac{\vec{\tilde{V}}\cdot\vec{F}_b}{B} + \vec{\tilde{V}}\cdot\vec{\hat{F}}_{\tau} + \rho\breve{T}\vec{\tilde{V}}\cdot\nabla\breve{s} \tag{12}$$

Details of the derivation are analogous to the steady-throughflow derivation (Mao and Dang, 2020) and hence are not presented here. Interested readers can refer to the references or the appendix.

From Equations (10) through (12), it is clear that the resultant governing equations for averaged flow quantities are similar to standard unsteady RANS equations, except the source terms on the right-hand side emerging from the average process. $\vec{F}_b$ and $\vec{\hat{F}}_{\tau}$ are body forces that require further modelling and $\vec{P}$ is the perturbation stemmed from the averaging over nonlinear terms. The following sections will discuss the formulations of body-force source terms.

FORMULATION OF BODY FORCES

There are two types of body forces in Equations (10) through (12). The $\vec{F}_{bs}$ represents the inviscid (pressure) force of the blade acting upon the flow; and the $\vec{\hat{F}}_{\tau}$ represents the loss induced by the blade row. Since they have rather different characteristics, hence they are modelled separately based on their physical representations.

Inviscid body force

Mathematically, the formulation of the inviscid body force resulting from the above derivation is as follows (circumferential component as an example)

$$F_{b\theta} = \frac{N}{2\pi r}\left[p\left(t,x,r,\theta_{\mathrm{p}}\right) - p(t,x,r,\theta_{\mathrm{s}})\right] \tag{13}$$

Essentially the circumferential inviscid body force is the instantaneous pressure difference at the blade surface. Apparently, from the perspective of modelling, Equation (13) is not directly applicable as the instantaneous pressure distributions on blade surfaces are not available to blade designers in the preliminary design phase whatsoever. Therefore, an alternative formulation of an inviscid body force is required for further usage.

Recall that in steady throughflow, the inviscid body force is formulated as a function of the mean angular momentum (Damle et al., 1997; Mao and Dang, 2020), That is

$$rF_{b\theta,steady} \approx \nabla\cdot B\rho\vec{V}\Gamma^{*}_{steady} + B\frac{\partial p}{\partial\theta} \tag{14}$$

Therefore, once users acquire the target angular momentum variation, Γ^{*}, one can construct the inviscid body force using Equation (14). However, for unsteady analysis, such a formulation is certainly not applicable as it misses the unsteady component of body force due to the unsteadiness in pressure at blade surfaces (i.e., Equation (13)). A simple method to relate the unsteady body force to the steady one is proposed by Longley (2007). Essentially, the unsteadiness induced body force can be reflected by the unsteadiness in angular momentum that is convected through the blade passage by the local flow. Hence, one can assume that the temporal variation of angular momentum is approximately the deviation of angular momentum from its mean (steady) value within the flow-through-passage time. That is

$$\frac{d\Gamma}{dt} = \frac{\Gamma_{steady} - \Gamma}{\tau} \tag{15}$$

The τ is the reference time of flow passing through the passage. Note that since the steady angular momentum is available, the instantaneous angular moment is obtainable. And the instantaneous inviscid body force becomes

$$rF_{b\theta} \approx \nabla \cdot B\rho\vec{V}\Gamma^{*} + B\frac{\partial p}{\partial \theta} \tag{16}$$

Viscous body force

Similar to the inviscid body force, the viscous body force for unsteady flows can also be acquired by relating the instantaneous viscous force to the steady one. Using the model proposed by Boseman and Marsh (1974) and the 3D correction by Mao and Dang (2020), the steady viscous body force can be written as

$$\vec{F}_{\tau,steady} = \begin{bmatrix} F_{\tau,x,steady} \\ F_{\tau,r,steady} \\ F_{\tau,\theta,steady} \end{bmatrix} = \begin{bmatrix} -\rho\mathcal{L}(x,r,\theta)\frac{\vec{W}}{|\vec{W}|}\cdot\vec{e}_x \\ -\rho\mathcal{L}(x,r,\theta)\frac{\vec{W}}{|\vec{W}|}\cdot\vec{e}_r \\ -\rho\mathcal{L}(x,r,\theta)\frac{\vec{W}}{|\vec{W}|}\cdot\vec{e}_\theta \end{bmatrix} \tag{17}$$

$$\mathcal{L}(x,r,\theta) = \frac{T}{|\vec{W}|}\vec{V}\cdot\nabla s^{*}_{steady} \tag{18}$$

The unsteady viscous force can be related to the steady force via the time lag relation for entropy. That is

$$\frac{ds}{dt} = \frac{\mathrm{s}_{steady} - \mathrm{s}}{\tau} \tag{19}$$

And the instantaneous viscous force is then

$$\mathcal{L}(t,x,r,\theta) = \frac{T}{|\vec{W}|}\vec{V}\cdot\nabla s^{*} \tag{20}$$

Computational Domain

The above equations are derived for the flow through the nozzle. For the turbine rotor, the governing equations are in the rotating frame. Corresponding derivations are analogous to the above derivations and the formulations of body forces are rather similar to those in the absolute frame.

Upon implementation, the computational domain is two annulus ducts interfaced at the intra-blade region. In general, the computational domain is “full-wheel” in the circumference (c.f. Figure 2). But since the physical blades are replaced with the body force sources, the computational cost is thus greatly reduced since the mesh size is much smaller compared to that in the authentic full-wheel simulation.

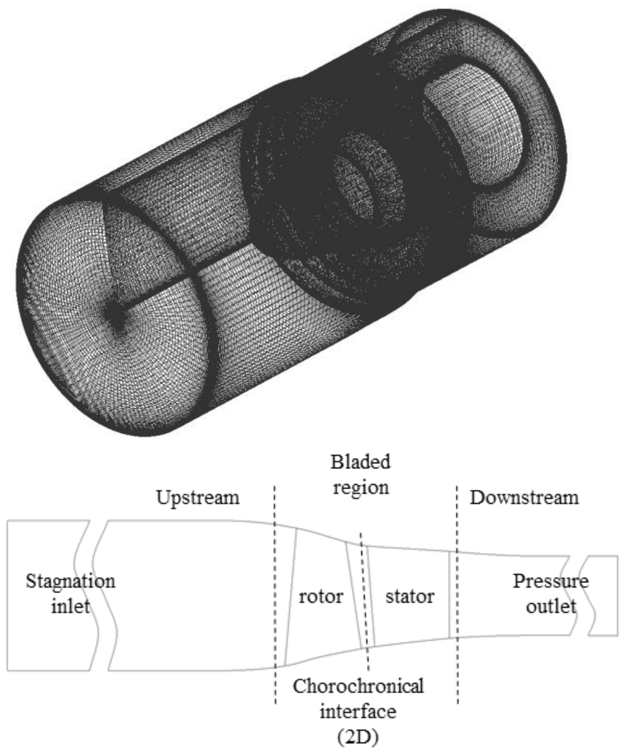

Figure 2 Computational domain: (up) 3D view; (down) meridional view

DISCUSSION

The above derivations are for 3D unsteady flows in general. On some specific occasions, the proposed method can be further simplified to axisymmetric formulations. Considering the source of unsteadiness, besides the small-scale unsteadiness that is not of the authors' interest, unsteadiness comes from two sources: boundary conditions and rotor-nozzle(stator) interactions. If the boundary conditions are clean and steady, then rotor-nozzle interactions are responsible for the unsteadiness within the flow field. For such flow configurations, the phase angle relation (Gerolymos, 2002) become very crucial. That is

$$\Phi\left(t,x,r,\theta+\frac{2\pi}{N}\right)=\Phi(t+\delta t,x,r,\theta) \tag{21}$$

Taking the continuity equation as an example, applying Equation (7) onto Equation (1), yields

$$\frac{\partial B\hat{\rho}}{\partial t}+\frac{\partial B\hat{\rho}\check{V}_x}{\partial x}+\frac{1}{r}\frac{\partial Br\hat{\rho}\check{V}_r}{\partial r}+\frac{N}{2\pi rB}\left(\rho V_\theta\left(t,x,r,\theta+\frac{2\pi}{N}\right)-\rho V_\theta(t,x,r,\theta)\right)=0 \tag{22}$$

Combining Equations (21) and (22), one can obtain

$$\frac{\partial B\hat{\rho}}{\partial t}+\frac{\partial B\hat{\rho}\check{V}_x}{\partial x}+\frac{1}{r}\frac{\partial Br\hat{\rho}\check{V}_r}{\partial r}+\frac{N}{2\pi rB}\big(\rho V_\theta(t+\delta t,x,r,\theta)-\rho V_\theta(t,x,r,\theta)\big)=0 \tag{23}$$

Equation (23) is free of circumferential variations. Hence one can use only one meridional plane to simulate the flow. That is, for a configuration where the inflow and outflow conditions are steady, an unsteady two-row stage flow field can be simulated by standard axisymmetric throughflow in two frames (rotating and stationery for the configuration in Figure 1), interfaced with the chorochronical interface proposed by Gerolymos (2002). The simulation can capture, in theory, unsteadiness associated with a length scale larger than one blade pitch. Such simulations will reduce the computational cost drastically and has rather large potentials in future unsteady analysis and modelling studies.

CONCLUSIONS

This paper presents a novel theory for unsteady analysis with the throughflow method. The governing equations for throughflow quantities are derived from standard unsteady RANS equations with no assumption. Hence one should expect the proposed method is valid for all the turbomachineries. The resultant equations contain body forces, which are formulated using the first-order time lag relation. Formulations of body forces are rather neat as they are related information of the corresponding steady flow field, hence it is implementation friendly if one wishes to implement the proposed model to any existing unsteady RANS solvers. Upon discussion, the authors also find out that for clean inflow and outflow conditions, with the chorochronical interface concept, the modelling of large-scale (lower than blade passing frequency) unsteadiness, which originates from rotor-stator interactions in turbomachineries, can be further simplified to unsteady 2D axisymmetric simulations , which can further reduce the computational cost for quality unsteady analysis.

NOMENCLATURE

B	=	blockage factor
D	=	viscous dissipation
δ	=	Dirac function
$\delta\tau$	=	phase lag
F	=	body forces
G	=	gate fuction (Eq. (8))
Γ	=	angular momentum
h	=	enthalpy
$\mathcal{L}$	=	loss body force magnitude
N	=	blade number
P	=	pertubation
p	=	pressure
ρ	=	density
Q	=	heat transfer
θ	=	circumferential coordinates
R	=	specific gas constant
r	=	radial coordinates
S	=	source terms
s	=	entropy
T	=	temperature
τ	=	reference time
ϑ	=	reference circumferential location
V	=	absolute velocity
W	=	relative velocity
ω	=	rotational speed
x	=	axial coordinates

Subscripts

$\wedge$	=	moving average
$\smile$	=	ρ-weighted moving average

Subscripts

0	=	stagnation quantities
b	=	blade body force
i	=	free index ($i = x, r, \theta$)
p	=	pressure surface
s	=	suction surface
θ	=	in circumferential direction
r	=	in radial direction
τ	=	viscous (loss) body force
x	=	in axial direction

REFERENCES

Adamczyk, J. J. (1984.11). Model equation for simulating flows in multistage turbomachinery. NASA TM-86869.

Casey, M., and Robinson, C. (2010). A New Streamline Curvature Throughflow Method for Radial Turbomachinery. Journal of Turbomachinery, 132 (3), pp. 031021-031021-10. doi:10.1115/1.3151601.

Damle, S. V., Dang, T. Q., and Reddy, D. R. (1997) Throughflow Method for Turbomachines Applicable for All Flow Regimes. Journal of Turbomachinery, 119 (2), , pp. 256-262. doi:10.1115/1.2841108.

Dawes, W. N. (1988). Development of a 3D Navier–Stokes Solver For Application to All Types of Turbomachinery. ASME Paper No. 88-GT-70.

Day, I. J. (1993). Stall Inception in Axial Flow Compressors. Journal of Turbomachinery, 115(1): 1-9.

Denton, J. D. (1975). A Time Marching Method For Two and Three Dimensional Blade to Blade Flows. ARC R&M 3775.

Denton, J. D. (1992) .The Calculation of Three-Dimensional Viscous Flow through Multistage Turbomachine. ASME Journal of Turbomachinery 114(1): 18–26.

Envia, Edmane , A. G. Wilson , and D. L. Huff .(2004). Fan Noise: A Challenge to CAA. International Journal of Computational Fluid Dynamics, 18 (6), pp. 471-480. doi: 10.1080/10618560410001673489

Gerolymos, G. A. (2002). Analysis and Application of Chorochronic Periodicity in Turbomachinery Rotor/Stator Interaction Computations. Journal of Propulsion and Power, 18(6): 1139-1152.

Gerolymos, G. A. (2013). Filtered Chorochronic Interface as A Capability for 3-D Unsteady Throughflow Analysis of Multistage Turbomachinery. International Journal of Computational Fluid Dynamics, 27(2): 100-117.

Guo, J, Hu, J, Wang, X, & Xu, R. (2020). A Three-Dimensional Unsteady Through-Flow Model for Rotating Stall in Axial Compressors. Proceedings of the ASME Turbo Expo 2020: Turbomachinery Technical Conference and Exposition. Volume 2A: Turbomachinery. Virtual, Online. September 21–25, 2020.

He, L. (1990). An Euler Solution for Unsteady Flows around Oscillating Blades. ASME Paper, 89-GT-279, The 34th international gas turbine and aeroengine congress and exhibition, Toronto, Canada, June, 1989, also, ASME Journal of Turbomachinery 1990, 112(4).

He, L. (1997). Computational Study of Rotating-Stall Inception in Axial Compressors. Journal of Propulsion and Power, 13(1): 31-38.

He, L. (2010). Fourier Methods for Turbomachinery Applications. Progress in Aerospace Sciencs, 46(8): 329-341.

Hyndman, R J. (2011) Moving Averages. International Encyclopedia of Statistical Science: 866-869. doi: 10.1007/978-3-642-04898-2_380

Jennions, I. K., and Stow, P. (1985a). A Quasi-3D Turbomachinery Blade Design System: Part I: Throughflow Analysis. Journal of Engineering for Gas Turbines and Power, 107 (2), pp. 301-307. doi:10.1115/1.3239715.

Jennions, I. K., and Stow, P. (1985b). A Quasi-3D Turbomachinery Blade Design System: Part II: Computerized System. Journal of Engineering for Gas Turbines and Power, 107 (2), pp. 308-314. doi:10.1115/1.3239716.

Longley, J. P. (2007). Calculating Stall and Surge Transients. In Turbo Expo: Power for Land, Sea, and Air, 47950: 125-136.

Lyman, F. A. (1993). On the Conservation of Rothalpy in Turbomachines. ASME 1992 International Gas Turbine and Aeroengine Congress and Exposition.

Mao, Y. and Dang, T. Q. (2020). A Three-Dimensional Body-Force Model For Nacelle-Fan Systems Under Inlet Distortions. Aerospace Science and Technology, 106: 106085.

Mazzawy, R. S. (1977). Multiple Segment Parallel Compressor Model for Circumferential Flow Distortion. Journal of Engineering for Power, 99 (2), pp. 288-296.

Novak, R. A. (1967). Streamline Curvature Computing Procedures for Fluid-Flow Problems. Journal of Engineering for Power, 89 (4), pp. 478-490. doi:10.1115/1.3616716.

Peters, A., Spakovszky, Z. S., Lord, W. K., and Rose, B. (2015). Ultrashort Nacelles for Low Fan Pressure Ratio Propulsors. Journal of Turbomachinery, 137(2): 021001-021001-14.

Righi, M., Pachidis, V., Könözsy, L., Pawsey, L. (2018). Three-Dimensional Through-Flow Modelling of Axial Flow Compressor Rotating Stall and Surge. Aerospace Science and Technology, 78, pp. 271-279.

Spurr, A. (1980). The Prediction of 3D Transonic Flow in Turbomachinery Using a Combined Throughflow and Blade-To-Blade Time Marching Method. International Journal of Heat and Fluid Flow, 2 (4), pp. 189-199. doi:10.1016/0142-727X(80)90013-2

Sturmayr, A., and Hirsch, C. (1999). Throughflow Model for Design and Analysis Integrated in a 3D Navier-Stokes Solver. Proceedings of the Institution of Mechanical Engineers, Part A: Journal of Power and Energy, 213 (4), pp. 263-273. doi:10.1243/0957650991537608

Wu, C. H. (1952.1). A General Theory of Three-Dimensional Flow in Subsonic and Supersonic Turbomachines of Axial, Radial and Mixed-Flow Types. NACA TN-2604.

APPENDIX – Moving Average

For an arbitrary quantity Φ inside a stationary blade, it can always be decomposed as

$$\Phi = \widehat{\Phi} + \Phi''' = \breve{\Phi} + \Phi'''' \qquad \text{(A.1 1)}$$

Next, we need to derive how the moving average operator interacts with different derivative operators. For spatial derivatives, say the radial derivative, according to the definition of moving average, one can have

$$\frac{\partial\widehat{\Phi}}{\partial r} = \frac{N}{2\pi B}\int_{\vartheta}^{\vartheta+\frac{2\pi}{N}} G\frac{\partial \Phi}{\partial r}d\theta = \frac{N}{2\pi B}\left[\underline{\frac{\partial}{\partial r}\int_{\vartheta}^{\vartheta+\frac{2\pi}{N}} G\Phi d\theta} - \underline{\int_{\vartheta}^{\vartheta+\frac{2\pi}{N}} \Phi\frac{\partial G}{\partial r}d\theta}\right] \quad \text{(A.1 2)}$$

The first underscored term is the radial derivative of the moving-averaged quantity. Note that

$$\frac{\partial G}{\partial r} = \left[\delta(\theta-\theta_s)\frac{\partial\theta_s}{\partial r} - \delta(\theta-\theta_p)\frac{\partial\theta_p}{\partial r}\right] \quad \text{(A.1 3)}$$

Substituting equation (A.1 3) to equation (A.1 2), it can be obtained that

$$\frac{\partial\widehat{\Phi}}{\partial r} = \frac{1}{B}\frac{\partial B\widehat{\Phi}}{\partial r} - \frac{N}{2\pi B}\left[\Phi(x,r,\theta_s)\frac{\partial\theta_s}{\partial r} - \Phi(x,r,\theta_p)\frac{\partial\theta_p}{\partial r}\right] \quad \text{(A.1 4)}$$

Similarly, for axial derivatives, one can have

$$\frac{\partial\widehat{\Phi}}{\partial x} = \frac{1}{B}\frac{\partial B\widehat{\Phi}}{\partial x} - \frac{N}{2\pi B}\left[\Phi(x,r,\theta_s)\frac{\partial\theta_s}{\partial x} - \Phi(x,r,\theta_p)\frac{\partial\theta_p}{\partial x}\right] \quad \text{(A.1 5)}$$

For the circumferential derivative, the moving-averaged circumferential derivative can be decomposed as

$$\frac{\partial\widehat{\Phi}}{\partial \theta} = \frac{N}{2\pi B}\int_{\vartheta}^{\vartheta+\frac{2\pi}{N}} G\frac{\partial \Phi}{\partial \theta}d\theta = \frac{N}{2\pi B}\left[\underline{\int_{\vartheta}^{\vartheta+\frac{2\pi}{N}} \frac{\partial G\Phi}{\partial \theta}d\theta} - \underline{\int_{\vartheta}^{\vartheta+\frac{2\pi}{N}} \Phi\frac{\partial G}{\partial \theta}d\theta}\right] \quad \text{(A.1 6)}$$

For the first underscored term, using the Leibniz rule, it can be expanded as

$$\int_{\vartheta}^{\vartheta+\frac{2\pi}{N}} \frac{\partial G\Phi}{\partial \theta}d\theta = \frac{\partial}{\partial\vartheta}\int_{\vartheta}^{\vartheta+\frac{2\pi}{N}} G\Phi d\theta - \int_{\vartheta}^{\vartheta+\frac{2\pi}{N}} \frac{\partial G\Phi}{\partial \vartheta}d\theta = \frac{\partial}{\partial\vartheta}\int_{\vartheta}^{\vartheta+\frac{2\pi}{N}} G\Phi d\theta \quad \text{(A.1 7)}$$

The second underscored term in equation (A.1 6) becomes

$$\int_{\vartheta}^{\vartheta+\frac{2\pi}{N}} \Phi\frac{\partial G}{\partial \theta}d\theta = \Phi(x,r,\theta_p) - \Phi(x,r,\theta_s) \quad \text{(A.1 8)}$$

Substituting equations (A.1 7) and (A.1 8) back to equation (A.1 6), one can have

$$\frac{\partial\widehat{\Phi}}{\partial \theta} = \frac{1}{B}\frac{\partial B\widehat{\Phi}}{\partial \vartheta} - \frac{N}{2\pi B}\left[\Phi(x,r,\theta_p) - \Phi(x,r,\theta_s)\right] \quad \text{(A.1 9)}$$

Then one can apply these properties of the moving average operator onto a conservative expression, that is

$$\begin{aligned}
&\frac{\partial\widehat{\rho\Phi}}{\partial t} + \frac{\partial\widehat{\rho\Phi V_x}}{\partial x} + \frac{1}{r}\frac{\partial \widehat{r\rho\Phi V_r}}{\partial r} + \frac{1}{r}\frac{\partial\widehat{\rho\Phi V_\theta}}{\partial\theta} \\
&\quad = \frac{\partial\widehat{\rho\Phi}}{\partial t} + \frac{1}{B}\frac{\partial B\widehat{\rho\Phi V_x}}{\partial x} + \frac{1}{rB_s}\frac{\partial rB\widehat{\rho\Phi V_r}}{\partial r} + \frac{1}{B_s}\frac{\partial B\widehat{\rho\Phi V_\theta}}{\partial\vartheta} \\
&\quad - \frac{N}{2\pi B}\left[(\rho\Phi)|_{\theta_s}\left(V_x\frac{\partial\theta_s}{\partial x} + V_r\frac{\partial\theta_s}{\partial r} - \frac{V_\theta}{r}\right)\Big|_{\theta_4}\right. \\
&\quad \left. - (\rho\Phi)|_{\theta_p}\left(V_x\frac{\partial\theta_p}{\partial x} + V_r\frac{\partial\theta_p}{\partial r} - \frac{V_\theta}{r}\right)\Big|_{\theta_3}\right]
\end{aligned} \quad \text{(A.1 10)}$$

The last two terms in equation (A.1 10) are zero because

$$\left(V_x\frac{\partial\theta_{3,4}}{\partial x} + V_r\frac{\partial\theta_{3,4}}{\partial r} - \frac{V_\theta}{r}\right)\Big|_{\theta_{3,4}} = 0 \quad \text{(A.1 11)}$$

Then equation (A.1 10) reduces to

$$\frac{\partial\widehat{\rho\Phi V_x}}{\partial x} + \frac{1}{r}\frac{\partial \widehat{r\rho\Phi V_r}}{\partial r} + \frac{1}{r}\frac{\partial\widehat{\rho\Phi V_\theta}}{\partial\theta} = \frac{\partial\widehat{\rho\Phi}}{\partial t} + \frac{1}{B}\frac{\partial B\widehat{\rho\Phi V_x}}{\partial x} + \frac{1}{rB}\frac{\partial rB\widehat{\rho\Phi V_r}}{\partial r} + \frac{1}{B}\frac{\partial B\widehat{\rho\Phi V_\theta}}{\partial\vartheta} \quad \text{(A.1 12)}$$